Electronic Supplementary Information for

Mesoporous Au film with surface sulfur modification for efficient ammonia electrosynthesis

Mei Zhang, Ziqiang Wang,* Hongjie Yu, Shengqi Wang, You Xu, Xiaonian Li,

Liang Wang* and Hongjing Wang*

State Key Laboratory Breeding Base of Green-Chemical Synthesis Technology, College of Chemical Engineering, Zhejiang University of Technology, Hangzhou 310014, P. R. China

*Corresponding authors' E-mails: zqwang@zjut.edu.cn; wangliang@zjut.edu.cn; hjw@zjut.edu.cn

Production determination. Indophenol indicator method was adopted to estimate the concentration of ammonia in the Na_2SO_4 electrolyte after electrolysis for 2 h.[1,2] Typically, 500 μL of NaOH solution (0.32 M) containing sodium salicylate (0.4 M), 50 μL of NaClO solution (0.05 M) containing NaOH (0.75 M), and 50 μL of $C_5FeN_6Na_2O$ (1 wt%) dissolved to 10 mL of deionized water were added into 4 mL of electrolyte in the dark for 1 h. Then, absorbance was determined by an ultraviolet-visible (UV-vis) spectrophotometer (Shimadzu UV-2450) using indophenol blue method at λ = 685 nm. The absolute calibration curve was obtained using the standard NH_4Cl solution with a series of NH_4^+ concentrations. All the measurements were conducted at least for 3 times for checking the reproducibility, and the data deviation was within 0.2%. The NH_3 yield (r_{NH3}) and Faradaic efficiency (FE) were calculated by using the following equations:

$$r_{NH3} = (c_{NH3} \times V)/t \times m \quad (1)$$

$$FE = 3F \times n_{NH3}/ Q \quad (2)$$

where c_{NH3} (μg mL^{-1}) is the mass concentration of produced NH_3, V (mL) is the volume of the Na_2SO_4 electrolyte, t (h) is the reduction reaction time, m (mg) is the loading mass of catalysts, F (96485 C mol^{-1}) is the faraday constant, n_{NH3} (mol) is the mole of produced NH_3 and Q (C) is the total electric quantity in the whole NRR process.

The concentration of hydrazine was spectrophotometrically determined by using Watt-Chrisp spectrophotometric method.[3] A mixed solution containing 5.99 g of 4-dimethylaminobenzaldehyde ($C_9H_{11}NO$), 30 mL of HCl and 300 mL of ethanol was used as the color reagent. Specifically, 5 mL of electrolyte was mixed with 5 mL of color reagent at room temperature. After standing for 10 min, the absorbance of the resulting solution was measured at a wavelength of 458 nm. The

concentration-absorbance curve was calibrated by using the standard N_2H_4 solution under various concentrations ranging from 0.2 to 2.0 mg mL^{-1}. All the measurements were taken at least for three times in order to check the reproducibility, and the data deviation was within 0.3%.

Detection of NO_3^- ions: The NO_3^- ions were detected according to the reported literature.[4] The standard solutions of NO_3^- ions were prepared as follows.

1) 100 μg mL^{-1} stock: 0.1 g of pre-dried KNO_3 was added into 1 L of deionized water.

2) 5 μg mL^{-1} stock: 5 mL of the above 100 μg mL^{-1} stock was mixed with deionized water to 100 mL.

3) The 0.1, 0.2, 0.5, 1.0, 1.5, 2.0, 2.5, 3.0, 4.0 and 5.0 mL solutions were separately added into the test tubes, which was mixed with deionized water to 5 mL, and 0.1, 0.2, 0.5, 1.0, 1.5, 2.0, 2.5, 3.0, 4.0 and 5.0 μg mL^{-1} standard solutions were finally obtained.

The concentration of the NO_3^- in Na_2SO_4 solution can be determined by UV-vis spectrophotometer at the wavelength of 220 nm. In a typical procedure, 5 mL of electrolytes were added to the test tubes followed by addition of 0.1 mL of 1.0 M HCl. After shaking up and standing for 5 min, the concentration of NO_3^- was measured using UV-vis spectrophotometer. The standard curve for NO_3^- ions was plotted using the standard solutions.

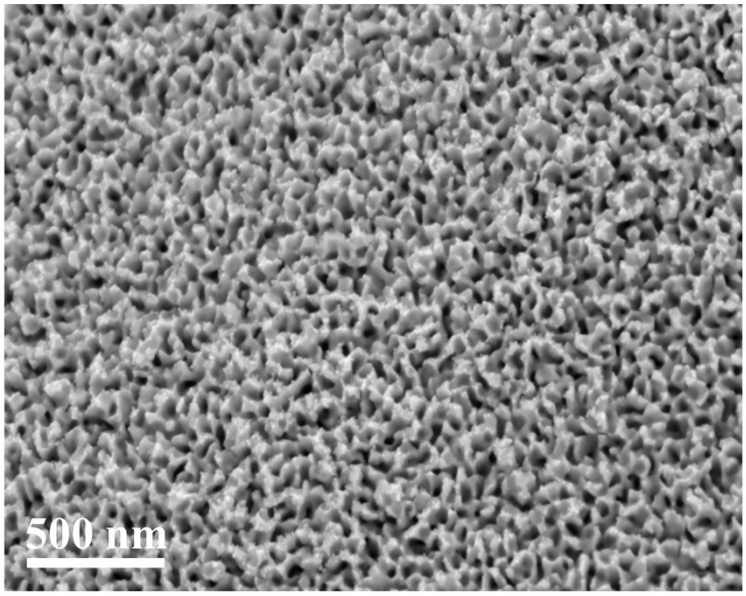

Fig. S1 The SEM image of mAu film/NF.

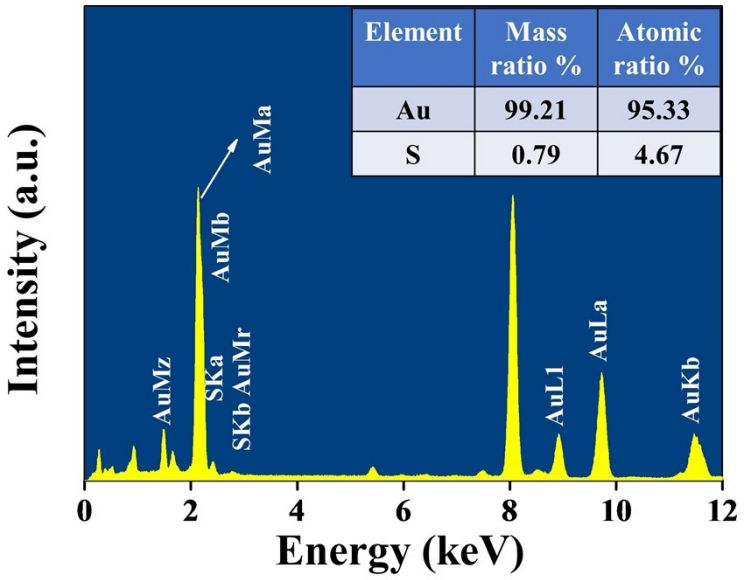

Fig. S2 The EDX spectrum of S-mAu film.

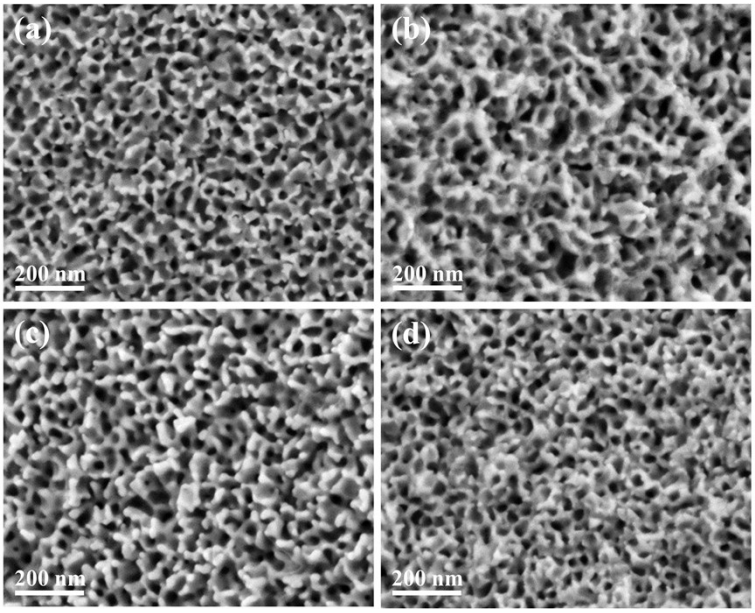

Fig. S3 SEM images of the S-mAu film/NF with different S doping amounts: (a) 0 mg, (b) 10 mg, (c) 20 mg (d) 40 mg of sulfur.

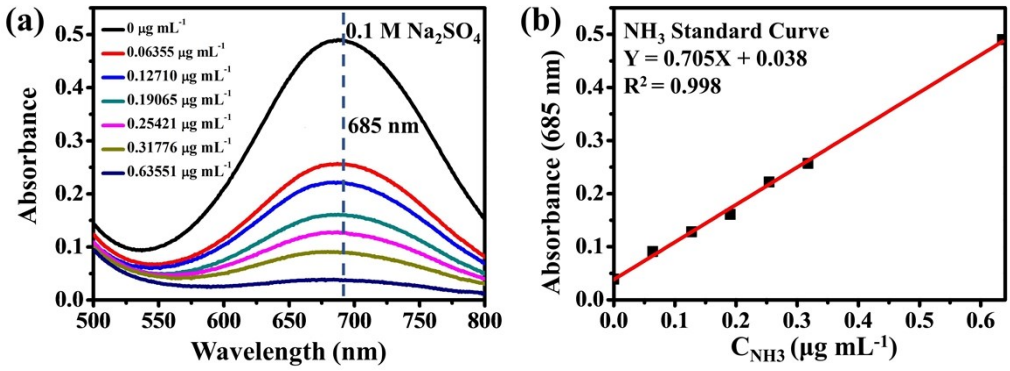

Fig. S4 (a) UV-Vis absorption spectra of standard NH_3 solutions with color development and (b) the corresponding calibration curve. The fitting curves shows good linear relation of absorbance with NH_3 concentration ($Y = 0.705X + 0.038$, $R^2 = 0.998$) of three times independent calibration curves.

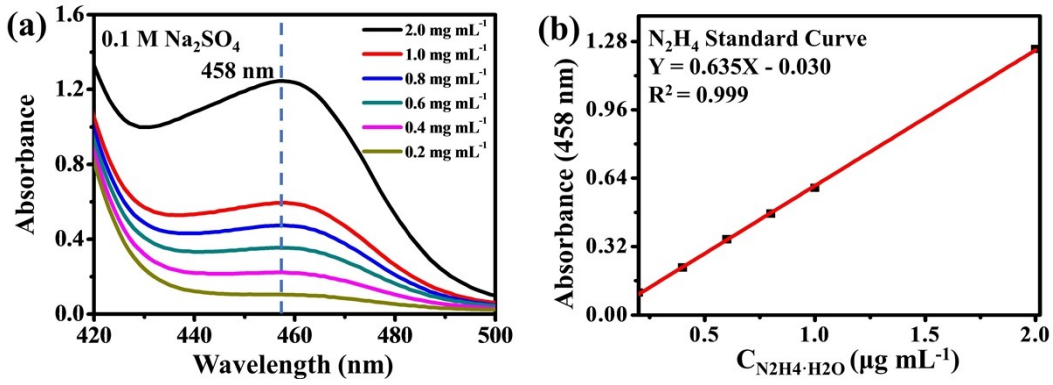

Fig. S5 (a) UV-Vis absorption spectra of standard N_2H_4 solutions with color development and (b) calibration curve used for estimation of N_2H_4 concentration. The fitting curve shows good linear relation of absorbance with N_2H_4 concentration (Y = 0.635X - 0.030, R^2 = 0.999) of three times independent calibration curves.

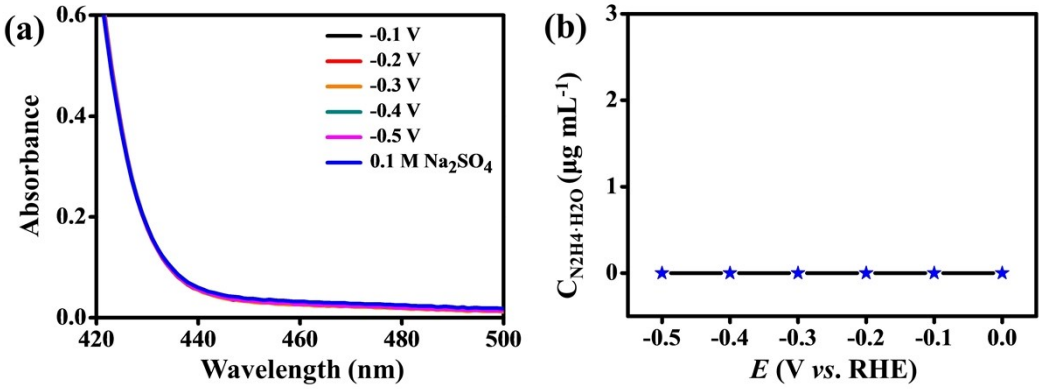

Fig. S6 (a) The UV-vis absorption spectra and (b) corresponding yields of N_2H_4 at selected potentials.

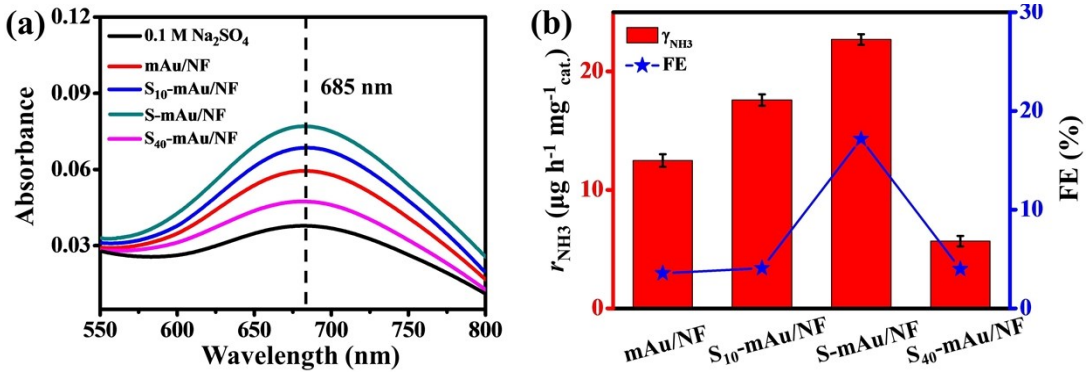

Fig. S7 (a) UV-vis absorption spectra of different catalysts at -0.2 V for 2-h electrolysis under ambient conditions, and (b) the NH_3 yields and Faraday efficiencies at selected potentials.

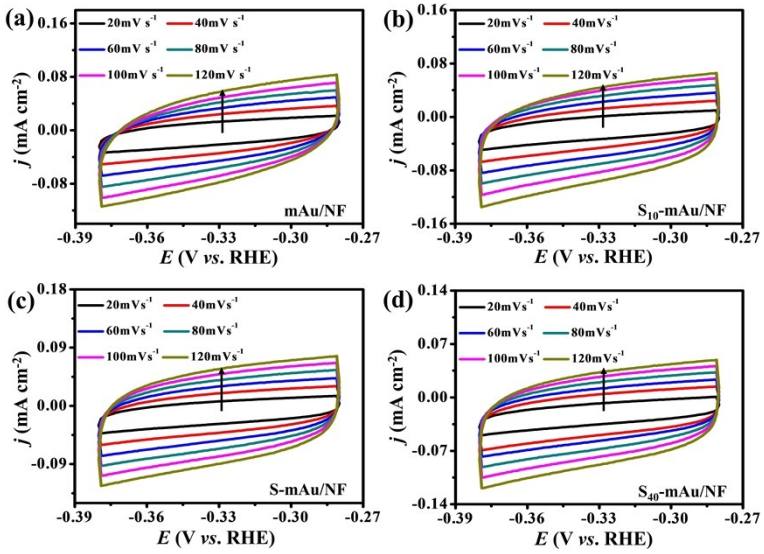

Fig. S8 Cyclic voltammograms for different catalysts in 0.1 M Na_2SO_4 solution with potential ranges from -0.35 to -0.45 V.

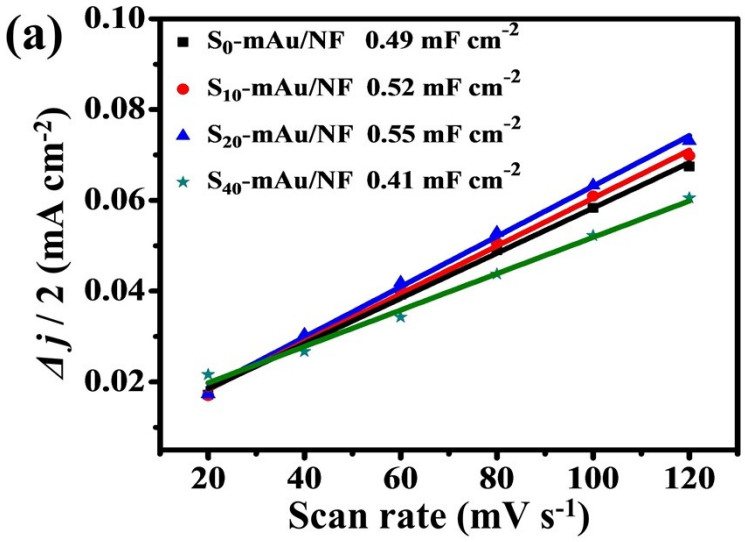

Fig. S9 (a) Charging current density differences plotted against scan rates.

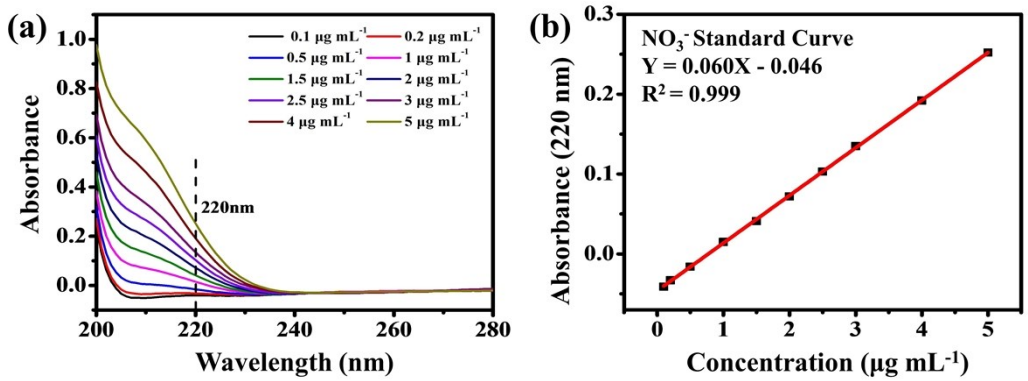

Fig. S10. (a) UV-vis spectra for various concentrations of KNO_3 solutions. (b) Calibration curve used for calculating the concentration of nitrate.

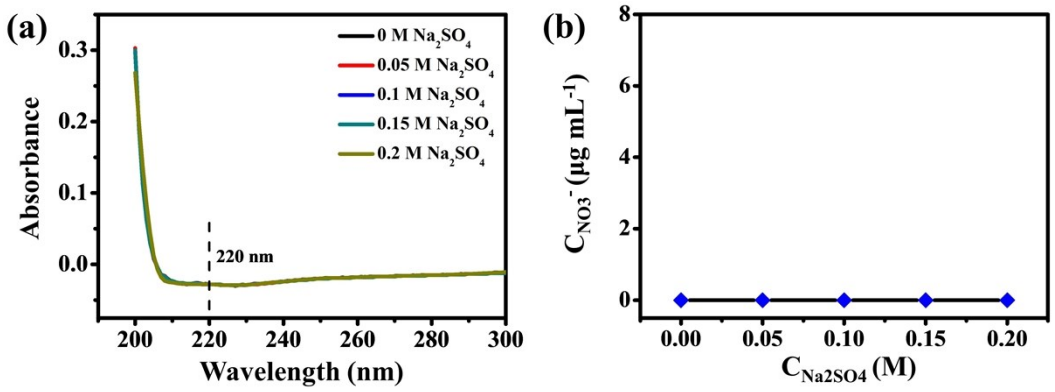

Fig. S11. (a) UV-vis adsorption spectra for determining the concentration of NO_3^- ions in Na_2SO_4. (b) The concentration of NO_3^- ions in various concentrations of Na_2SO_4.

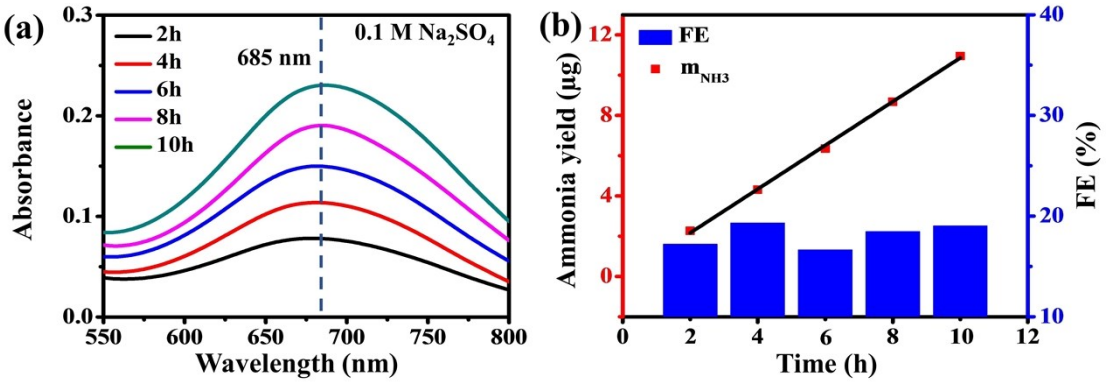

Fig. S12 (a) UV-vis absorption spectra of solution with different electrolysis times at -0.2 V and (b) the linear relationship between the m_{NH3} and the electrolysis time.

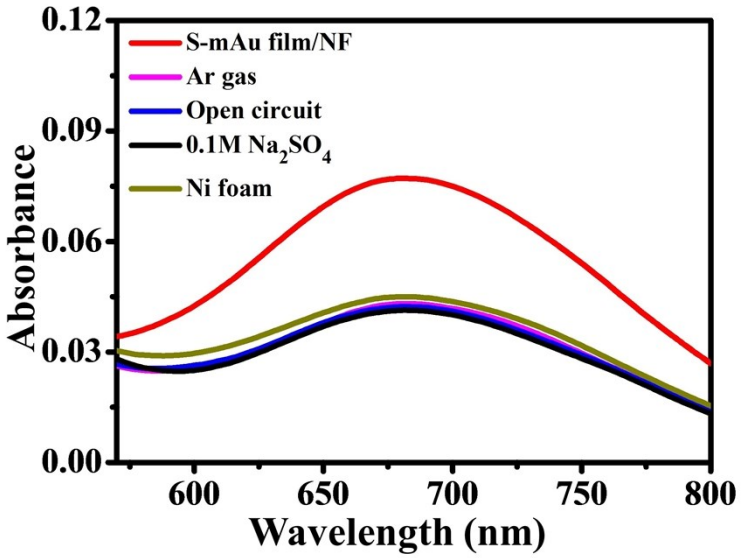

Fig. S13 The absorbance of the electrolytes at -0.2 V for 2 h under different reaction conditions.

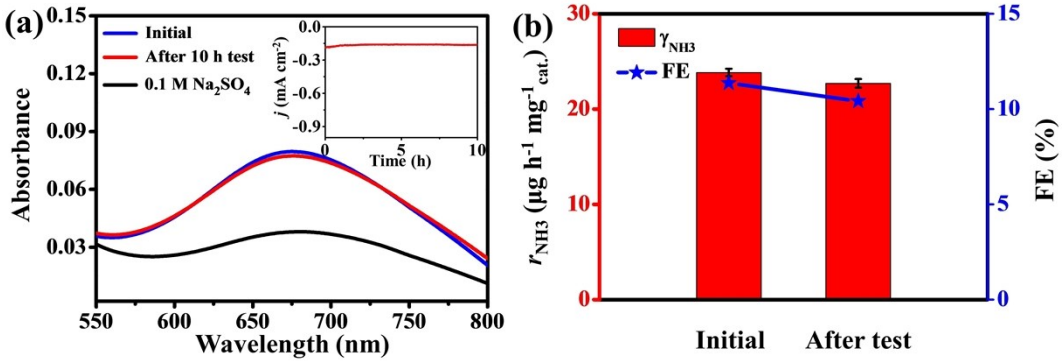

Fig. S14 (a) The comparison of UV-vis absorption spectra of the electrolytes before and after electrolysis for 10 h, and the inset shows the time-dependent measurements. (b) Corresponding the NH_3 yields and Faraday efficiencies of the S-mAu film/NF.

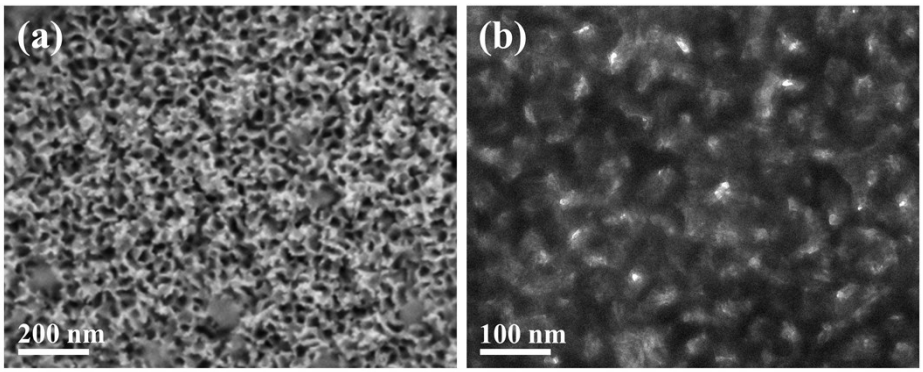

Fig. S15 The SEM (a) and TEM images (b) of the S-mAu film/NF after durability measurement.

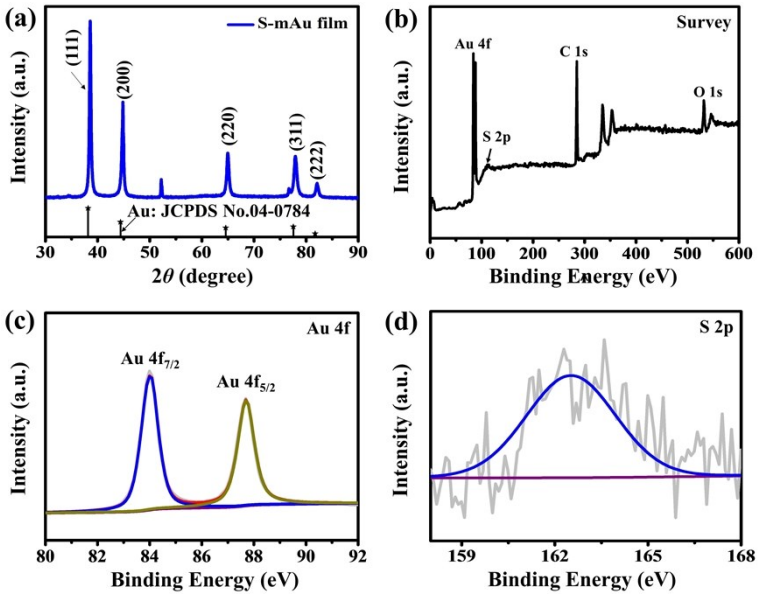

Fig. S16 (a) Wide-angle XRD patterns and (b) the XPS survey spectrum and high-resolution XPS spectra of (c) the Au 4f and (d) S 2p core levels for S-mAu film after durability measurement.

Table S1 Summary of the representative reports on electrocatalytic NRR at ambient conditions.

Catalyst	Electrolyte	r_{NH3}	FE(%)	Ref.
S-mAu film/NF	**0.1 M Na_2SO_4**	**22.7 μg h^{-1} $mg^{-1}_{cat.}$ (4.54 μg h^{-1} cm^{-2})**	**17.2**	**This work**
PdCuIr-LS	0.1 M Na_2SO_4	13.43 μg h^{-1} $mg^{-1}_{cat.}$	1.84	[5]
pAu/NF	0.1 M Na_2SO_4	9.42 μg h^{-1} cm^{-2}	13.36	[6]
Au flowers	0.1 M HCl	25.57 μg h^{-1} $mg_{cat.}^{-1}$	6.05	[7]
Au@SnO_2	0.1 M HCl	21.9 μg h^{-1} $mg_{cat.}^{-1}$	15.2	[8]
Au/TiO_2	0.1 M HCl	21.4 μg h^{-1} $mg_{cat.}^{-1}$	8.11	[9]
a-Au/CeO*x*–RGO	0.1 M HCl	8.3 μg h^{-1} $mg^{-1}_{cat.}$	10.10	[10]
Au/WO_3-x	0.1 M KOH	23.15 μg h^{-1} $mg_{cat.}^{-1}$	14.72	[11]
Au-Fe_3O_4 NPs	0.1 M KOH	21.42 μg h^{-1} cm^{-2}	10.54	[12]
Au/C	0.1 M KOH	17.49 μg h^{-1} mg_{Au}^{-1}	5.79	[13]
Ru@MXene	0.1 M KOH	2.3 μmol h^{-1} cm^{-2}	13.13	[14]
Au NRs	0.1 M KOH	1.65 μg h^{-1} cm^{-2}	3.88	[15]
Hollow gold nanocage	0.5 M $LiClO_4$	3.9 μg cm^{-2} h^{-1}	14.8	[16]

References

1. C. Patton and S. Crouch, *Anal. Chem.*, 1977, **49**, 464-469.
2. D. Zhu, L. Zhang, R. Ruther and R. Hamers, *Nat. Mater.*, 2013, **12**, 836-841.
3. A. Ensafi, M. Sadeghie and F. Emamei, *J. Anal. Chem.*, 1999, **54**, 1024-1027.
4. Li, L.; Tang, C.; Yao, D.; Zheng, Y.; Qiao, S.-Z. Electrochemical Nitrogen Reduction: Identification and Elimination of Contamination in Electrolyte. ACS Energy Letters 2019, **4** (9), 2111-2116, DOI: 10.1021/acsenergylett.9b01573.
5. R. Kumar, Z. Wang, C. Li, A. Kumar, H. Xue, Y. Xu, X. Li, L. Wang and H. Wang, *J. Mater. Chem. A*, 2019, **7**, 3190-3196.
6. H. Wang, H. Yu, Z. Wang, Y. Li, Y. Xu, X. Li, H. Xue and L. Wang, *Small*, 2019, **15**, 1804769.
7. Z. Wang, Y. Li, H. Yu, Y. Xu, H. Xue, X. Li, H. Wang and L. Wang, *ChemSusChem*, 2018, **11**, 3480-3485.
8. P. Wang, Y. Ji, Q. Shao, Y. Li and X. Huang, *Sci. Bull.*, 2020, **65**, 350-358.
9. M. Shi, D. Bao, B. Wulan, Y. Li, Y. Zhang, J. Yan and Q. Jiang, *Adv. Mater.*, 2017, **29**, 1606550.
10. S. Li, D. Bao, M. Shi, B. Wulan, J. Yan and Q. Jiang, *Adv. Mater.*, 2017, **29**, 1700001.
11. Y. Li, P. Yan, J. Chen, Y. Ren, Y. Zhou, T. Ge and Q. Xu, *Chem. Commun.*, 2019, **55**, 13307-13310.
12. J. Zhang, Y. Ji, P. Wang, Q. Shao, Y. Li and X. Huang, *Adv. Funct. Mater.*, 2020, **30**, 1906579.
13. C. Chen, C. Liang, J. Xu, J. Wei, X. Li, Y. Zheng, J. Li, H. Tang and J. Li, *Electrochim. Acta*, 2020, **335**, 135708.
14. A. Liu, M. Gao, X. Ren, F. Meng, Y. Yang, Q. Yang, W. Guan, L. Gao, X. Liang and T. Ma, *Nanoscale*, 2020, **12**, 10933-10938.
15. D. Bao, Q. Zhang, F. Meng, H. Zhong, M. Shi, Y. Zhang, J. Yan, Q. Jiang and X. Zhang,

Adv. Mater., 2017, **29**, 1604799.

16. M. Nazemi, S. Panikkanvalappil and M. El-Sayed, *Nano Energy*, 2018, **49**, 316-323.